Journal of Control, Automation and Electrical Systems
https://doi.org/10.1007/s40313-023-01020-6

Fractional-Order Tilt Integral Derivative Controller Design Using IMC Scheme for Unstable Time-Delay Processes

Anjana Ranjan[1] · **Utkal Mehta**[1]

Received: 10 February 2023 / Revised: 26 June 2023 / Accepted: 28 June 2023

Abstract
The paper proposes a modified IMC-based Smith predictor (SP) control method for unstable time-delay processes. A novel design method to tune the parameters of a fractional-order tilt integral derivative controller has been developed using fractional-order IMC filter and process model parameters. The tuning parameters of the fractional-order filter are calculated from the new robustness index and desired performance constraint. The expected performance constraint satisfies good setpoint tracking and optimal control signal. The significant feature of the presented method is that the fractional IMC-SP structure provides a better outcome without adding much computational complexity. For a given robustness index, the optimal controller, which minimizes the performance constraint, the combination of control effort and integral time squared error, helps calculate the two tuning parameters. The benefit does verify under parameters' uncertainties, external load disturbances and noise. The comparative study with various numerical examples from recently reported methods shows better overall servo and regulatory performances.

Keywords Unstable process · Fractional-order control · Internal model control (IMC) · Smith predictor (SP) · Robustness · Load disturbance

1 Introduction

Controlling open-loop unstable processes such as heating boilers or batch chemical reactors is challenging due to poles in the right-half s-plane and large time constants. Moreover, the slow process causes additional phase lag, making the closed-loop system unstable. The dead time delays may occur due to transportation, recycle loops, measurement lags, some computation times or communication lags. Furthermore, the strong load disturbances result in breaking the balance of input–output. The tuning of controllers to stabilize these processes and disturbance rejection will become a critical task for process engineers.

The PID (Proportional Integral Derivative) controllers are the most essential control algorithm, due to their simple structure, and lower order, and it helps in managing both transient and steady-state responses, and it is summarized by Rakesh et al. (2021). A concise review of the complexity and cost dilemma in PID controller tuning and discussed about the proposal to minimize the dilemma of complexity and cost that has become associated with tuning the three main parameters in one of the recent work by Somefun et al. (2021). PID has some limitations apart from being one of the best controllers in a control action system. It does not perform well in the case of optimal control. Also, it shows some structural limitations for the process having considerable dead time. Thus, the Smith predictor (SP) is a superior technique to deal with significant time delays. Nevertheless, the typical SP structure does not give desired closed-loop responses. To improve the performance, recently Ranjan and Mehta (2023b) have proposed a modified SP technique with multiple controllers in the structure.

A modified form of SP with three controllers was reported earlier by Rao and Manickam (2008) for a second-order unstable process. Later, Uma and Rao (2014) proposed a modified SP for non-minimum phase unstable second-order time delay processes with and without a zero. Their methods used a direct synthesis approach for set-point tracking and load disturbance rejection controllers. It was seen that

✉ Anjana Ranjan
anjanasarath85@gmail.com

Utkal Mehta
utkal.mehta@usp.ac.fj

[1] Electrical and Electronics Engineering, The University of the South Pacific, Laucala Campus, Suva, Fiji

Published online: 15 July 2023

the method requires a set-point weighting to reduce overshoots. Later, the works presented by Mehta and Rojas (2017) and Mehta and Kaya (2017) with hybrid combinations of SP with a sliding mode control to deal with significant time delay, overshoots and load disturbance issues. Also, a modified SP using three controllers was proposed by Ajmeri and Ali (2017). Again, the method used a direct synthesis and has a single tuning parameter. In general, it was found that an extra low-pass filter was necessary to achieve good robustness. A simplified IMC-based modified SP for unstable lag-dominated first-order process was presented by Karan and Dey (2020). But, there was a single tuning parameter for stabilizing, setpoint tracking and load disturbance rejection. The above literature concludes that the previous approaches have complex structural tuning, less immune to load disturbances and parameter perturbations. Most recently, a review article on Internal-Model-Control (IMC) methods presented to discuss the open challenges and future motivations by Ranjan et al. (2023). In addition, a generalized desired dynamic equational (G-DDE) PID was developed by Gengjin et al. (2022) to solve control problems of high-order open-loop unstable systems. Recently, the issues of dynamic modeling and control of manipulator with a flexible joint was presented by Bilal et al. (2017). Later Bilal et al. (2023a) studied an active disturbance rejection control law (ADRC) for the control of robotic manipulators. Furthermore, Bilal et al. (2023b) investigated the trajectory tracking and vibration control of rotary flexible joint manipulator with parametric uncertainties.

In recent years, fractional-order control has been attracting significant attention. Even though it has more than 300 years of narrative and deep-rooted mathematical concepts, the current research on this domain has come up with exciting outcomes. The fractional-order resulted more accurate and precise in reproducing the behavior of physical processes and robust performances than classical approaches (Padula & Visioli, 2015; Mehta et al., 2023). Although IMC-based methods are simple and provide robustness, the improvement can notice with a fractional-order filter. Recently, researchers have worked on fractional-order IMC control (FOIMC) for the height control of a conical tank nonlinear system (Vavilala et al., 2020) and for higher-order systems (Saxena & Biradar, 2022). The fractional-order approach in the parallel cascade scheme with the SP is also presented for stable, unstable and integrating plus time delay processes (Pashaei & Bagheri, 2020). However, this scheme consists of a complex tuning of three controllers.

There are notable methods in the literature to suggest improved performance for controlling unstable processes. Among them, the recent fractional PI-PD structure provided better results using stability boundary and weighted geometrical center methods developed by Ozyetkin (2018). In the same way, Onat (2019) proposed a PI-PD controller for unstable processes. From the stability boundary locus, the controller parameters can be obtained using the centroid of the convex stability region. The studies with IMC-PID structure by Vanavil et al. (2014), Begum et al. (2018), Begum et al. (2020) and Begum (2022) showed merits over many active methods developed at that time. For a set of unstable, integrating and inverse response type plants, a new design strategy was suggested by Raja and Ali (2021) using classical PI-PD controllers. Bingi et al. (2018) compared various forms of PID and fractional-order PID (FOPID) structures. It was proven the FOPID resulted in less overshoot and faster settling time compared to all forms of PID structures. Then, the fractional IMC-based hybrid dual loop strategy was developed by Kumar and Raja (2022) and Kumari et al. (2021) for unstable plants. A new fractional IMC filter was further developed recently by Ranjan and Mehta (2023a) for series cascade unstable plants.

The literature suggested that it was essential to look at the load disturbance performance while improving the setpoint tracking in unstable time-delay processes. The methods have either more than two controllers in structure, difficulty in tuning parameters, or complex designing steps until recently presented schemes. Say, for example, a graphical tuning approach with FOPID has five different design requirements (Dwivedi & Pandey, 2021). Moreover, it can be seen from the relevant literature that the majority of designs fail to eliminate the overshoot (Begum et al., 2020) or to reduce settling time (Vanavil et al., 2014; Bingi et al., 2018). The load disturbance rejection also seems to be poor in some methods (Bingi et al., 2018; Ajmeri & Ali, 2017; Uma & Rao, 2014). Further, the design of the setpoint controller focuses solely on the intended closed-loop performance, whereas load disturbance in other stated approaches appears to be slower.

Looking into the above constraints, the novelties of the paper are listed below:

- This research presents a modified IMC-based SP configuration for an unstable process. Even if the controller contains a fractional-order integrator and derivative, the new structure is less complex in a tuning.
- For the first time, an IMC-based fractional TID controller for setpoint tracking and external load disturbance rejection is developed.
- Two tuning parameters, namely fractional-order and fractional filter time constant, are obtained using a novel robustness index and required performance constraint.
- Numerical studies examined the impact of load disturbances, measurement noises and perturbations on the dynamic responses of the system, with linear and nonlinear benchmark plant models.

In summary, the presented scheme works for unstable first- and second-order plants with one or two unstable poles.

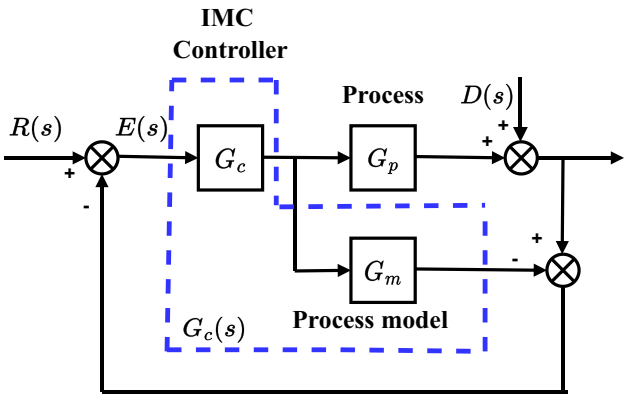

Fig. 1 Typical structure of IMC

Quantitative analysis shows that the results exceed the previous works. A case study on a nonlinear continuously stirred reactor is verifying the present strategy in a real-time scenario.

The paper is organized as follows. The background of IMC and fractional-order tilt integral derivative (FOTID) are introduced in Sect. 2; the proposed structure and its controller design are explained in Sect. 3. A detailed explanation of how the tuning parameters are calculated is discussed in Sect. 4, and their robustness and stability are described in Sect. 5. The verification of this method is described in Sect. 6, followed by conclusions in Sect. 7.

2 Background Study

2.1 The General IMC Control System

Fig. 1 depicts the IMC and its corresponding single-loop control mechanism. Assume G_p is the process, G_m is a process model, and Q is the IMC main controller. In addition, R, Y, and D represent the setpoint, process output, and load disturbance inputs, respectively. The fundamental principle behind IMC design is to use PID or a higher-order form as the feedback controller. Before introducing the proposed method with a fractional-filter IMC-SP, the most typical procedure has been outlined for the reference. According to IMC theory (Ranjan et al., 2023), the process model G_m may be split into two parts as,

$$G_m(s) = G_m^+(s)G_m^-(s) \tag{1}$$

where, $G_m^+(s)$ represents all time delays and unstable zeros (non-invertible) and $G_m^-(s)$ represents the minimum phase elements (invertible). The aim is to keep the controller at $Q(s) = G_m^-(s)^{-1}$. The user-specified filter is then chosen to satisfy the robustness criterion. The low-pass filter is used to reduce the consequences of process model mismatch. According to the extensive study by Nath et al. (2021), the common IMC filter was chosen as,

$$f(s) = \frac{1}{(\lambda s + 1)^n} \tag{2}$$

for better setpoint tracking. Here, λ is a tuning parameter known as the closed-loop time constant, which affects the speed of response. The integer order n is selected such that the controller $Q(s)$ is always proper. Thus, $Q(s)$ can be written as

$$Q(s) = f(s)G_m^-(s)^{-1}. \tag{3}$$

This filter was further improved to ensure enhanced disturbance rejection (Shamsuzzoha & Lee, 2008; Begum et al., 2017, 2020). Such filter's modification can employ with an extra tuning and complexity. Now, solving the inner loop as seen from Fig. 1, the relationship between the feedback controller $G_c(s)$ and $Q(s)$ can be described using,

$$G_c(s) = \frac{Q(s)}{1 - G_m^-(s)Q(s)}. \tag{4}$$

Finally, the output relationship from the closed-loop control with the IMC structure is,

$$Y(s) = \frac{G_pG_c}{1 + G_c(G_p - G_m)}R + \frac{1 - G_mG_c}{1 + G_c(G_p - G_m)}D. \tag{5}$$

In an ideal case, when the process is modeled accurately ($G_p = G_m$), (5) becomes $Y(s) = G_pG_cR(s) + (1 - G_mG_c)D(s)$. As per IMC theory, $Q(s) = G_m^{-1}(s)$, one can acquire complete control. It is simple when there is no process dead time or when a process is precisely recognized. This, however, is extremely vulnerable to modeling errors.

2.2 FOTID Controller

The well-known fractional-order PID controller requires the design of five parameters, most notably gains K_p, K_i, K_d and fractional-orders α and μ. It has been demonstrated in the literature that it can give more flexibility in achieving design control objectives. The TID controller is also from the fractional-order family and was introduced by Lurie (1994). This controller also provides more flexibility for desired performance. However, the structure is nearly identical to a well-accepted PID and has only four parameters. Only the proportional gain is replaced by the tilted gain (K_t) having a transfer function $1/s^{\frac{1}{n}}$, where n is a nonzero real number. The TID controller's standard transfer function is expressed as,

$$\text{TID} = K_t\frac{1}{s^{\frac{1}{n}}} + K_i\frac{1}{s} + K_ds \tag{6}$$

where, K_t is the tilted gain, K_i is the integral gain and K_d is the derivative gain. The value of n is a tuning parameter that should be between 2 and 3. When compared to other controllers, a TID controller provides more accurate tuning, faster disturbance rejection, and lowers parameter uncertainty. In recent years, there has been a surge in interest in this field of study. A robust 3DOF-TID by Guha et al. (2019) and ID-T reported by Ahmed et al. (2022) controllers, developed for load frequency problems in interconnected power systems were some of the works developed recently. The new fractional-order tilt derivative (TDD) controller presented by Ranjan and Mehta (2022) for all types of integrating processes. Together, FOTID scheme was proposed recently by Ranjan and Mehta (2023b) for cascade integrating processes. These have produced promising results when compared to previous schemes. Therefore, we have evaluated FOTID controller in the current investigations with simplifying tuning steps. The FOTID can be represented as,

$$\text{FOTID} = K_t \frac{1}{s^{\frac{1}{n}}} + K_i \frac{1}{s^{\alpha}} + K_d s^{\mu} \tag{7}$$

where, α and μ are positive real orders for integral and derivative, respectively. In this work, we utilize the IMC principle to create the FOTID as written in (7). Even though the controller appears to be sophisticated with three fractional orders, the goal is to create a simple tuning strategy.

3 Proposed FOIMC with Smith Predictor Structure

Figure 2 depicts the suggested control scheme. It is made up of the process $G_p(s)$. It is seen that $G_m(s)$ is the model transfer function of $G_p(s)$ without a delay. The following transfer function model, which has some generality, shall be considered as,

$$G_p(s) = \frac{K e^{-\theta s}}{(\tau_1 s \pm 1)(\tau_2 s - 1)} \tag{8}$$

where, K represents the process gain, τ_1 and τ_2 time constants and θ represents the time delay. The controller G_c is utilized for the stabilized plant $G_s(s)$. The stabilizing controller G_{c0} is used to stabilize the $G_p(s)$. We have considered the design method for three common forms of unstable process transfer function models. First, an unstable first-order process with dead time (UFOPDT) model is used; another unstable second-order process with dead time (USOPTD) model with one unstable pole, and the third with two unstable poles.

3.1 Designing Internal Stabilizing Controller G_{c0}

The stabilizing controller considered here is of the form

$$G_{c0} = K_{ps}\left(1 + \frac{T_{ds} s}{\eta T_{ds} s + 1}\right) \tag{9}$$

where K_{ps} is a proportional gain, T_{ds} is a derivative time constant, and η is a derivative filter constant. The value of η is a small constant and so, the derivative filter terms can be neglected in calculations hereafter. Note it is applied in all simulation studies. In the first case ($\tau_1 \neq 0, \tau_2 = 0$), the UFOPDT process G_p gives the model without delay as, $G_m^-(s) = \frac{K}{\tau_1 s - 1}$. In order to make the overall transfer function stable with G_m^-, the controller G_{c0} is enough for a proportional gain with greater than $1/K$ value as suggested by Tan et al. (2003). As seen from Fig. 2, the proportional controller G_{c0} is typically chosen such that $K K_{ps} > 1$ and $T_{ds} = 0$. Then, the P-controller from (9) can be designed as

$$G_{c0} = K_{ps} \geq \frac{1}{K} \tag{10}$$

By choosing $K_{ps} = \frac{2}{K}$, a stable model can be obtained using

$$\frac{G_m}{1 + G_m G_{c0}}, \tag{11}$$

and it is represented as $G_s(s)$ in Fig. 2. It is to note that the SP usually is more robust when considering a stable process model. Now, for the second-order unstable models, G_{c0} can be used as a simple PD controller. When a second-order unstable model ($\tau_1 \neq 0, \tau_2 \neq 0$) of the form $G_m^- = \frac{K}{(\tau_1 s+1)(\tau_2 s-1)}$ is considered, then by selecting $K K_{ps} = 2$ and $T_{ds} = \tau_1$, one unstable pole transfer function becomes stable in the loop. Same way, two unstable poles in the USOPDT model can be modified by taking $K_{ps} \to 0$ and $K K_{ps} T_{ds} > 0$. By selecting suitable values of K_{ps} and T_{ds}, one can make the unstable process model stable for controlling purposes.

3.2 Designing Main Controller G_c from IMC Approach

Firstly, consider G_p as a first-order unstable process. After stabilizing the model and removing the time-delay, one can obtain the model as,

$$G_s(s) = \frac{K}{\tau s + 1}. \tag{12}$$

Let us take the form of an IMC filter with fractional- order,

$$f(s) = \frac{1}{\lambda s^{\beta} + 1} \tag{13}$$

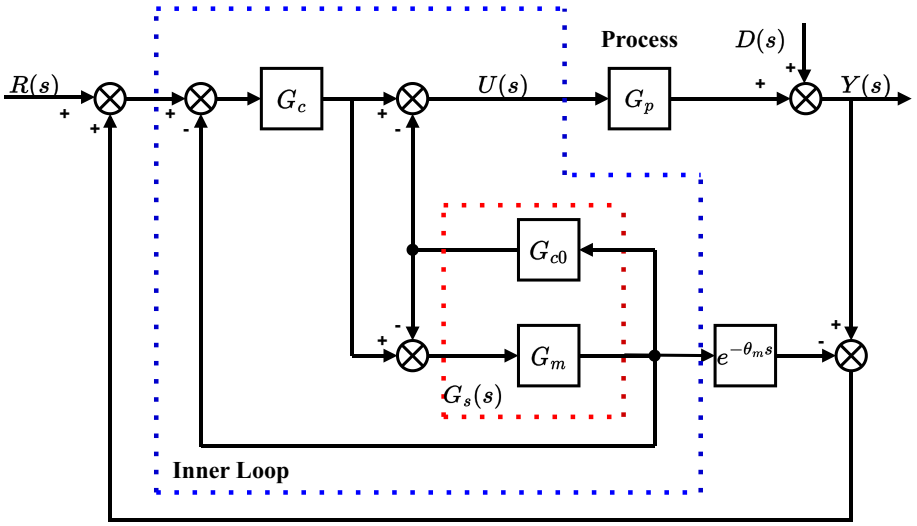

Fig. 2 Modified IMC-based Smith predictor for unstable time delay processes

where, λ represents a fractional filter time constant ($\lambda > 0$) and β is a positive real number, i.e., the fractional-order ($1 < \beta < 2$). We have only considered two tuning parameters in our method. After substituting (12) and (13), the resulting IMC controller $Q(s)$ can be obtained from (3) and is represented as,

$$Q(s) = \frac{\tau s + 1}{K} \frac{1}{\lambda s^{\beta} + 1}. \tag{14}$$

As per the IMC method, one can obtain the feedback controller, $G_c(s)$ from the stabilized model (12) and IMC controller (14). Substituting in (4), we get

$$G_c(s) = \frac{\tau s + 1}{\lambda K s^{\beta}}. \tag{15}$$

(15) can be arranged with respect to the fractional-order TI structure as,

$$G_c(s) = \frac{1}{\lambda K s^{\beta}} + \frac{\tau}{\lambda K s^{\beta - 1}}. \tag{16}$$

Comparing with (7), the parameters become

$$K_t = \frac{1}{\lambda K}; K_i = \frac{\tau}{\lambda K}; \beta = 1/n; \alpha = (\beta - 1). \tag{17}$$

In a similar way, for the USOPDT model, the IMC controller is obtained as,

$$Q(s) = \frac{(\tau_1 s + 1)(\tau_2 s + 1)}{K} \frac{1}{\lambda s^{\beta} + 1}. \tag{18}$$

And the feedback controller is,

$$G_c(s) = \frac{(\tau_1 s + 1)(\tau_2 s + 1)}{K \lambda s^{\beta}}. \tag{19}$$

After rearranging as per (7), $G_c(s)$ becomes

$$G_c(s) = \frac{1}{\lambda K} \frac{1}{s^{\beta}} + \frac{\tau_1 + \tau_2}{\lambda K} \frac{1}{s^{\beta - 1}} + \frac{\tau_1 \tau_2}{\lambda K} s^{2 - \beta} \tag{20}$$

Now, the FOTID gains in terms of process model parameters are,

$$K_t = \frac{1}{\lambda K}; K_i = \frac{\tau_1 + \tau_2}{\lambda K}; K_d = \frac{\tau_1 \tau_2}{\lambda K}; \beta = 1/n; \\ \alpha = (\beta - 1); \mu = (2 - \beta). \tag{21}$$

In summary, the controller design becomes simplified using model based. The main tuning parameters λ and β are required to calculate optimally as suggested in the following section.

4 Proposed Controller Design for Unstable Processes

This section specifies the critical tuning settings for the IMC-SP control structure given. The calculation of the performance index and tuning to alter the optimization priority between the two objectives are provided.

4.1 Performance Constraint with IMC-SP Structure

The closed-loop controlled system must process dynamics-insensitive while selecting controller parameters. From this, the approach is created to relate tuning parameters to maximum sensitivity. Aiming this point (Kumar & Hote, 2020), the new robustness index is defined by ξ for the new fractional-order filter in the IMC-SP structure. It also determines whether the controller is designed to be a tight control or smooth control. The required range of tightness or smooth-

ness may vary in the different process types selected. The other commonly used sensitivity measures are gain margin (A_m) and phase margin (ϕ_m). It is given by

$$A_m = \left| \frac{1}{L(j\omega_{pc})} \right| \tag{22}$$

$$\phi_m = \pi + \left[\arg L(j\omega_{gc}) \right] \tag{23}$$

where, ω_{pc}, phase crossover frequency, is the frequency at which the phase angle of the loop transfer function first reaches $-180°$ and ω_{gc}, gain crossover frequency, the frequency at which Nyquist curve has a magnitude of 1 (0 dB). In our case, the open-loop transfer function of the system in the inner loop is taken as

$$L(s) = G_c(s)G_s(s) \tag{24}$$

where, G_s represents the stabilized model. The value of ω_{gc} is considered as the bandwidth of the system. The typical values of ϕ_m is between 30° to 60° and A_m varies from 2 to 5. The range of ξ is chosen so that ϕ_m lies in its typical.
For chosen ξ, the condition of open-loop transfer function passing through point 'C' on the Nyquist plot in Fig. 3 can be expressed as,

$$L(j\omega)_{s=j\omega} = -1 + \frac{1}{\psi} e^{-j\psi}. \tag{25}$$

Also, the tangency condition at 'C' is,

$$\arg \frac{dL(j\omega)}{d\omega} = \frac{\pi}{2} - \psi \tag{26}$$

where, ψ is the angle of the line from the critical point $(-1, j0)$ to the tangent point and the negative real axis. Now, $L(s)$ for the inner loop becomes

$$L(s) = \frac{Q(s)G_s(s)}{1 - Q(s)G_s(s)}, \tag{27}$$

using (24) and (4). As it is understood from Fig. 2, instead of G_m^- we can take the stabilized model, $G_s(s)$. After substituting (12) and (14) in (27), one can write,

$$L(s) = \frac{1}{\lambda s^\beta}, \tag{28}$$

and using $s = j\omega$, it becomes

$$\begin{aligned} L(j\omega) &= \frac{1}{\lambda(j\omega)^\beta} = \frac{1}{\lambda[\omega^\beta \cos\frac{\beta\pi}{2} + j\omega^\beta \sin\frac{\beta\pi}{2}]} \\ &= \frac{1}{\lambda\omega^\beta}\left[\cos\frac{\beta\pi}{2} - j\sin\frac{\beta\pi}{2}\right]. \end{aligned} \tag{29}$$

Finally, using (29) into (25) and (26), the explicit relations,

$$\text{Re} : \frac{1}{\lambda\omega^\beta}\cos\frac{\beta\pi}{2} = \frac{1}{\xi}\cos\psi - 1 \tag{30}$$

$$\text{Im} : \frac{1}{\lambda\omega^\beta}\sin\frac{\beta\pi}{2} = \frac{1}{\xi}\sin\psi \tag{31}$$

$$\arg\frac{dL(j\omega)}{d\omega} = \frac{\pi}{2} - \psi \tag{32}$$

are obtained for finding tuning parameter values. It is to note that $\xi \in (0, 1)$. It is now possible to calculate two unknown parameters, λ and β using (30), (31) and (32).

Remark 1 The function fsolve from the MATLAB© Optimization Toolbox is utilized to obtain the optimal values. The equation solving function is setup with the trust-region-dogleg algorithm to calculate λ and β.

4.2 The Performance Constraint and Tuning Algorithm

The controller that focuses on setpoint tracking, actuator preservation, and maintaining robustness against model mismatch does not exist in real situations. So in this proposed tuning, the method is suggested considering the balance trade-off between those three objectives. The tuning aims to obtain optimal performance in setpoint tracking with reasonable control signal variations. The performance criterion is therefore defined by,

$$\underset{(\lambda,\beta,\xi)}{J_{\min}} = \nu \int_0^\infty |u(t)|\mathrm{d}t + (1-\nu)\int_0^\infty te(t)^2\mathrm{d}t \tag{33}$$

as the cost function. Here, $u(t)$ represents the control signal, $e(t)$ represents the error signal and ν is the weight coefficient. The index (33) is a combination of two criteria, namely total variations in input signal u and integral of time-weighted square error (ITSE) value. Note that $\nu \in [0, 1]$ can be used to adjust the optimization priority between two objectives. This can be a more attractive relation for the required trajectory tracking and energy consumption simultaneously. When the value of ν is closer to 0, the index behaves as more critical to setpoint tracking error and lesser control efforts. The index will be changed when ν becomes closer to 1. The major steps for the complete controller design are summarized in Table 1.

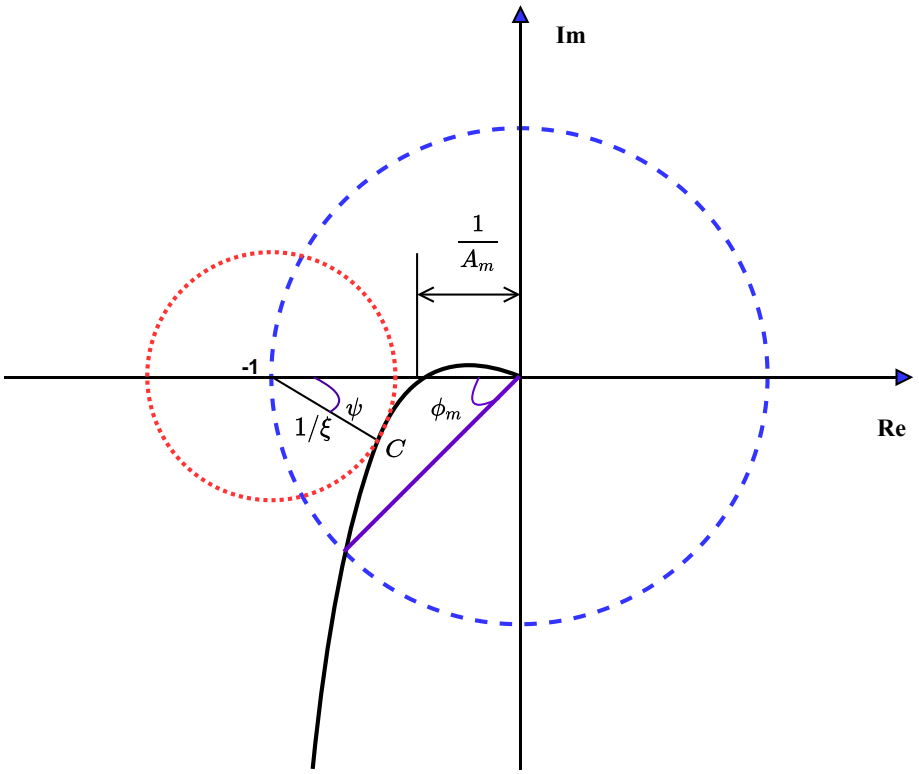

Fig. 3 Geometric interpretation of the constraint ξ

Table 1 The controller tuning steps

Step 1: Calculate bandwidth of G_s.
Step 2: For ξ between (0, 1), tabulate the calculated values of λ and β from (30), (31) and (32).
Step 3: Check the index value (33) and calculate ϕ_m from (23).
Step 4: Choose λ and β for minimum (33) and satisfied $\phi_m \leq 60°$.
Step 5: Obtain controller parameters using (17) or (21).

5 Robustness and Stability of the Closed-Loop System

Model uncertainties are common in the process industries. We took into account uncertainties in a process gain K and dead time θ.

As a well-known condition by Zhong-Ping and Tengfei (2018), a closed-loop system is stable only if,

$$\|\Delta_m(jw)T(jw)\| < 1 \forall \omega \in (-\infty, \infty) \tag{34}$$

where, $T(jw)$ is the complementary sensitivity function and $\Delta_m(jw)$ is the bound on the process multiplicative uncertainty. The process's uncertainty might be stated as

$$\Delta_m(jw) = |\frac{G_p(jw) - G_m(jw)}{G_m(jw)}| \tag{35}$$

where, $G_m(jw)$ is the model of the unstable process.

Assuming an uncertainty in K and θ, then the tuning parameters must be chosen so that,

$$||T(jw)||_\infty < \frac{1}{|(\frac{\Delta K}{K} + 1)e^{-\Delta\theta s} - 1|}. \tag{36}$$

Now, the proposed structure gives

$$T(jw) = \frac{G_c G_s e^{-jw\theta}}{1 + G_c G_s}. \tag{37}$$

For any unstable model discussed here, the complementary sensitivity function for the proposed scheme is given by,

$$T(jw) = \frac{e^{-jw\theta}}{\lambda(jw)^\beta + 1}. \tag{38}$$

In order to provide strong closed-loop performance, the sensitivity and complementary sensitivity functions must adhere

the constraints,

$$\|\Delta_m(jw)T(jw) + w_m(jw)(1 - T(jw))\| < 1 \tag{39}$$

where, $w_m(jw)$ is the uncertainty bound on the sensitivity function, which is given as $S(jw) = 1 - T(jw)$. As a result, tuning parameters must be chosen in such a way that the resultant controller meets the robust performance and stability constraints.

Remark 2 If Q and G_s are stable, then the feedback controller, given by G_c, will also be stable. Stability analysis methodologies created for integer-order plants cannot be used to fractional order models. Further investigation on the stability is provided by Ranjan and Mehta (2022) and shown that the closed-loop fractional controller becomes stable.

6 Illustration

The numerical illustration is carried out with several process models, and analysis has been done in a more detailed manner. Recent works presented by Begum et al. (2020, 2018), Vanavil et al. (2014), Onat (2019), Ozyetkin (2018), Bingi et al. (2018), Kumar et al. (2020), Ajmeri and Ali (2017) and Uma and Rao (2014) are considered for comparative analysis. To demonstrate performances, the values from the plant's output, such as settling time (t_s, sec), peak voltage (A_p), are calculated for each example studied. In addition to that the below mentioned performance metrics were also calculated in order to evaluate the performances.

- Integral Square Error (ISE) = $\int_0^\infty e^2(t)\mathrm{d}t$
- Integral Absolute Error (IAE) = $\int_0^\infty |e(t)|\mathrm{d}t$
- Integral Time Squared Error (ITSE) = $\int_0^\infty te^2(t)\mathrm{d}t$
- Integral Time Absolute Error (ITAE) = $\int_0^\infty |te(t)|\mathrm{d}t$

where, $e(t)$ represents the input to the controller. In general, the value of each index indicates the quality and speed of responses. All these indicators were separately calculated for both setpoint tracking and load disturbance rejection.

The percentage overshoot is a measure of how much the response exceeds the ultimate value following a step change in the set point. The settling time is the time required for the output to reach and steady within a given tolerance band. We considered the 5% band throughout all examples. Also, the white noise having a variance of 0.001 is added as a measurement noise to verify the control scheme's robustness against the noisy output.

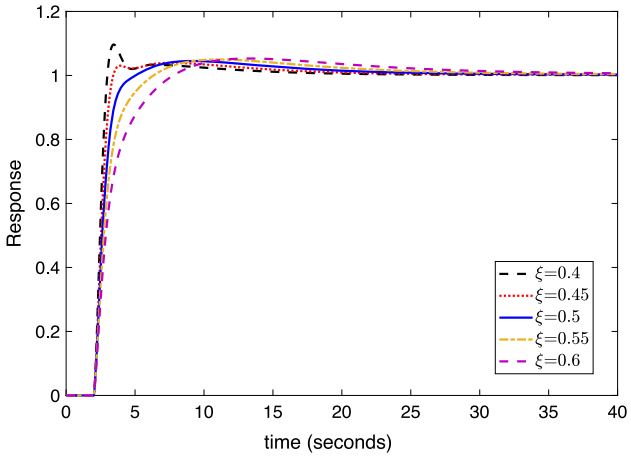

Fig. 4 Effects of ξ on setpoint responses

6.1 Example: 1

An unstable first-order plus time delay transfer system,

$$G_{p1}(s) = \frac{4}{4s - 1}e^{-2s} \tag{40}$$

is commonly studied in the literature. We have compared the presented method with PI-PD design by Onat (2019), a fractional order PI-PD (FOPI-PD) design by Ozyetkin (2018) and 2DOF PID as well as a fractional 2DOF FOPID by Bingi et al. (2018). The controller settings of Onat were obtained as $K_p = 0.107$, $K_i = 0.039$, $K_f = 0.439$ and $K_d = 0.341$ while for the same process, Ozyyetkin suggested a fractional controller as $K_p = 0.047$, $K_i = 0.022$, $K_f = 0.4092$ and $K_d = 0.211$ for $\lambda = \mu = 1.011$. Bingi et al. (2018) presented a comparative analysis of different types of PID structures. By taking the best responses, 2DOF PID as $K_p = 0.424$, $T_i = 30.959$, $T_d = 0.473$ and $\alpha = 0.025$ (where α is the derivative filter coefficient) and 2DOF FOPID with same controller's gains except the fractional-orders $\lambda = 0.980$ and $\mu = 0.650$ was used for performance verification.

Following our design, one can see the impact of ξ selection on output responses in Fig. 4. Then, the value of the performance constraint can be obtained as $\xi = 0.5$ for the optimal cost function using Figs. 5a and b. The obtained values of λ and β are 0.397 and 1.590, respectively. The stabilizing controller's gain was taken as $K_{ps} = 2.0$. Finally, the parameters in a fractional-order TI controller are $K_t = 0.630$, $K_i = 2.521$, $\beta = 1.590$ and $\alpha = 0.590$. A negative step disturbance of 0.1 is given at the output-side load. The results are plotted in Figs. 6a and b. The load disturbance rejection shows much improvement than others. The numerical values in Table 2 also depicted the method's performance than other recent works.

The robust performance is also observed by assuming a perturbation of 20% in process gain and process delay simul-

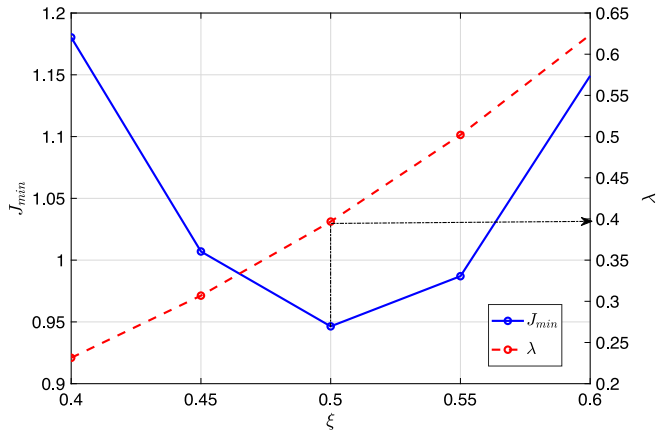

(a) Variation of λ and J_{min} with ξ for Example-1

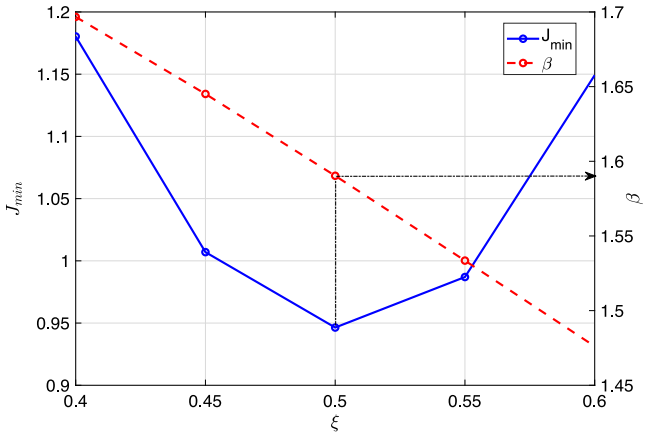

(b) Variation of β and J_{min} with ξ for Example-1

Fig. 5 Obtain the tuning parameters for Example-1

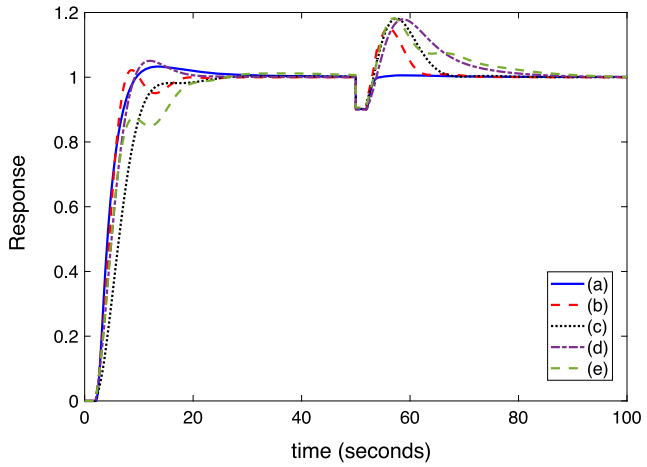

(a) Servo and Regulatory Responses

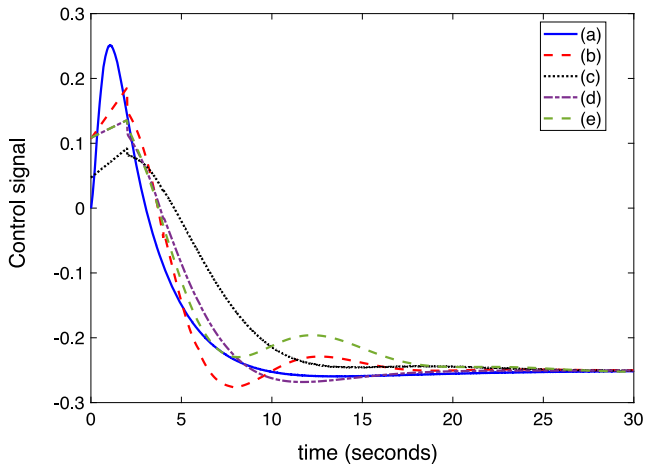

(b) Control signals

Fig. 6 Responses in Example-1, (a) Proposed, (b) Onat (2019), (c) Ozyetkin (2018), (d) 2DOF-PID by Bingi et al. (2018) and (e) 2DOF-FOPID by Bingi et al. (2018)

Table 2 Performance comparison for Example-1

Tuning methods	t_s	A_p	ITSE	IAE	ITAE	ISE
Setpoint tracking						
Proposed	8.017	1.032	0.312	1.038	6.086	0.118
Onat	6.970	1.021	7.920	4.864	14.985	3.813
Ozyetkin	11.930	0.984	15.080	6.799	27.995	5.143
Bingi et al. (PID)	12.444	1.050	17.774	4.908	58.223	1.329
Bingi et al. (FOPID)	17.172	0.982	11.091	6.326	29.788	4.247
Disturbance rejection						
Proposed	3.830	0.100	0.003	0.136	0.917	0.004
Onat	18.692	0.169	0.778	1.192	7.720	0.132
Ozyetkin	16.364	0.179	1.441	1.591	12.500	0.196
Bingi et al. (PID)	31.945	0.179	2.644	2.417	28.855	0.271
Bingi et al. (FOPID)	41.907	0.178	2.336	2.541	36.068	0.236

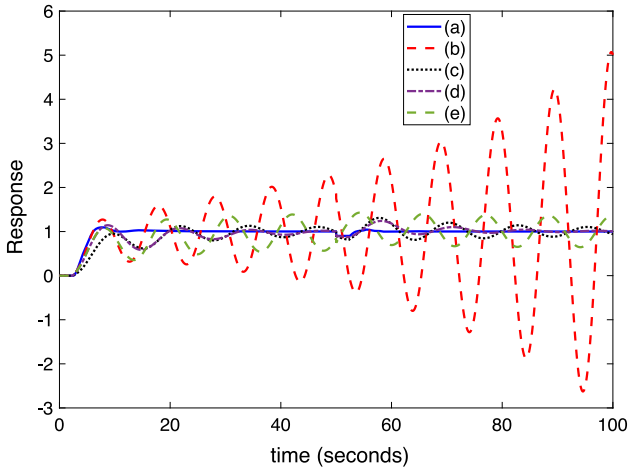

Fig. 7 Perturbation test 20% (process gain and delay) in Example-1, (a) Proposed, (b) Onat (2019), (c) Ozyetkin (2018), (d) 2DOF-PID by Bingi et al. (2018) and (e) 2DOF-FOPID by Bingi et al. (2018)

taneously. As seen from Fig. 7, the presented method is more robust than others and can resist significant parameter variations.

6.2 Example: 2

The familiar USOPTD plant studied by Kumar et al. (2020) and Begum et al. (2018) is presented here as

$$G_{p2}(s) = \frac{2}{(s-1)(3s-1)} e^{-0.25s}. \tag{41}$$

An IMC-PID controller was proposed by Kumar et al. (2020) in which the controller settings were calculated to be $K_c = 3.150$, $T_i = 1.553$, $T_d = 1.451$ and used set-point weighting parameter value of 0.2 in order to remove the excessive overshoot. For the above process model, the IMC-PID settings reported by Begum et al. (2018) were $K_c = 4.491$, $T_i = 1.625$, $T_d = 1.272$ and a set-point filter of the form $\frac{0.7768s+1}{1.9476s^2+1.5536s+1}$ also added to deal with overshoot. Again, the presented method is used to verify the performance. For a process (41), the performance constraint is considered upto a certain range that satisfies the conditions of ϕ_m (Table 1). The graphical plots are shown in Fig. 8a, b for suitable tuning parameters. The obtained tuning parameters are $\lambda = 0.299$, $\beta = 1.343$, and then, FOTID setting is $K_t = 1.673$, $K_i = 6.695$, $K_d = 5.022$, $\alpha = 0.343$ and $\mu = 0.657$. A setpoint filter of the form $F_s = 1/(s+1)$ is added in order to improve the smoothness of the response. The stabilizing controller's gains are chosen as $K_{ps} = 0.01$, $T_{ds} = 400$ and $\eta = 10^{-4}$ as per procedure from Sect. 3.1. A positive step disturbance of 0.1 is considered at the 20 s in order to study load disturbances. The closed-loop responses as well as control signals are shown in Fig. 9a and b. For checking the system robustness, the steady state gain, as well as process delay, is changed to 20% in the worst direction. From the perturbed responses shown in Fig. 10a and b, it shows no oscillations, even though the plant model is perturbed. In addition to that magnitude of complementary sensitivity function, $T(jw)$ with bound on multiplicative uncertainty, Δ_m for different perturbations is shown in Fig. 11. The robust stability margin decreases with an increase in perturbation. As it crosses 80%, the controller failed to satisfy the robust stability and robust performance condition as mentioned in (34). Hence, 70% is the recommended allowable perturbation for the given second-order plant.

The numerical values measured from the setpoint and after load disturbances are tabulated in Table 3. It shows that the new method can perform better compared with other methods.

6.3 Example: 3

A second-order process with one unstable pole is considered as,

$$G_{p3}(s) = \frac{1}{(s-1)(0.5s+1)} e^{-1.2s}. \tag{42}$$

Ajmeri and Ali (2017) used a modified Smith predictor structure with three controllers. Their method had a lead-lag compensator with parameter values, $\alpha_c = 0.628$ and $\beta_c = 0.429$, setpoint tracking PI with settings, $K_{c1} = 0.452$ and $T_{i1} = 4.371$ and load disturbance rejection PID with lead-lag filter with $K_{c2} = 1.091$, $T_{i2} = 69.553$ and $T_{d2} = 0.529$, filter parameters $\alpha_s = 0.6$ and $\beta_s = 0.019$. In addition, a low-pass filter of the form $G_f(s) = 1/(\theta s+1)$ to improve system robustness and a setpoint filter $F_f(s) = 1/(T_{i1}s+1)$ to remove overshoot were included in the structure. Thus, their method requires several controllers for unstable process control. Uma and Rao (2014) method presented a modified Smith predictor with two controllers, namely, setpoint tracking PID with filter as $K_{cs} = 1.496$, $K_{is} = 0.103$, $K_{ds} = 0.821$ and $\beta_s = 0.429$ and load disturbance PID with lead-lag filter as $K_{cd} = 1.192$, $K_{id} = 0.039$, $K_{dd} = 0.594$ and $\alpha_d = 0.6$ and $\beta_d = 0.011$. It shows their structure also depends on more tuning parameters.

Unlike the proposed approach, a designer could easily choose one parameter value ξ. For the given process, the performance constraint from the optimal cost function is calculated as $\xi = 0.72$ as shown in Fig. 12a and b. Then, tuning parameters are obtained as $\lambda = 0.597$ and $\beta = 1.343$ to satisfy the minimum cost function. The controller values obtained as $K_t = 1.676$, $K_i = 2.513$, $K_d = 0.838$, $\alpha = 0.343$ and $\mu = 0.657$. The stabilizing PD controller is $G_{c0} = 2(0.5s+1)$. The setpoint filter $F_s = 1/(1.5s+1)$ is considered to reduce the undesirable overshoots. A positive load disturbance of 0.05 is given at the output load. The servo

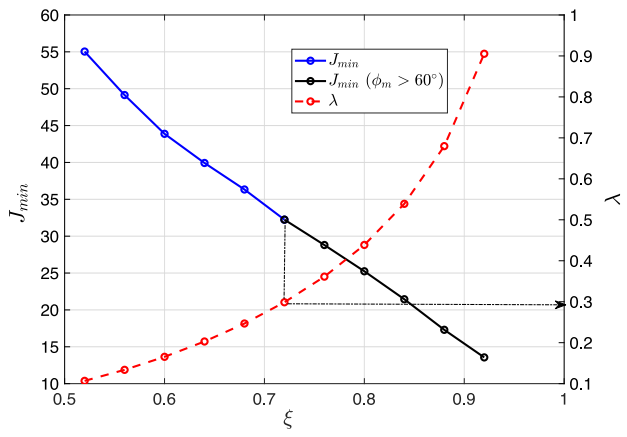

(a) Variation of λ and J_{min} with ξ for Example-2

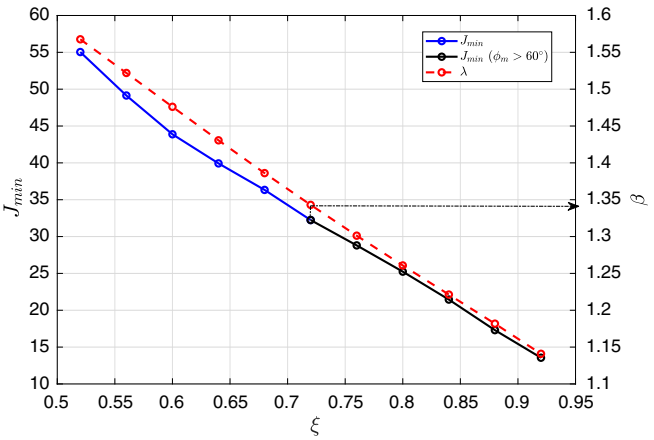

(b) Variation of β and J_{min} with ξ for Example-2

Fig. 8 Obtain the tuning parameters for Example-2

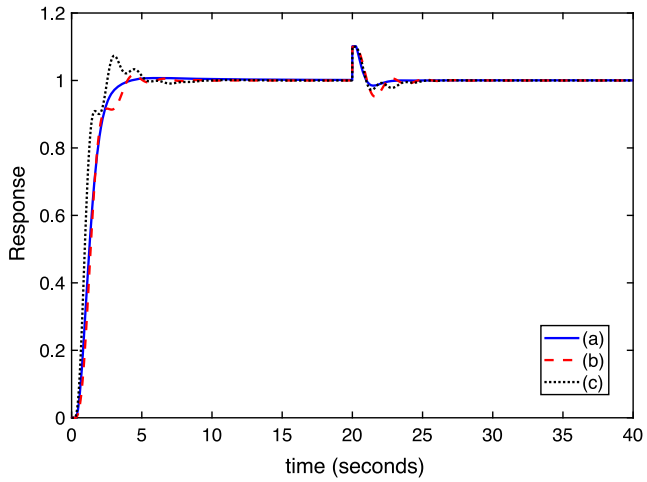

(a) Servo and Regulatory Responses

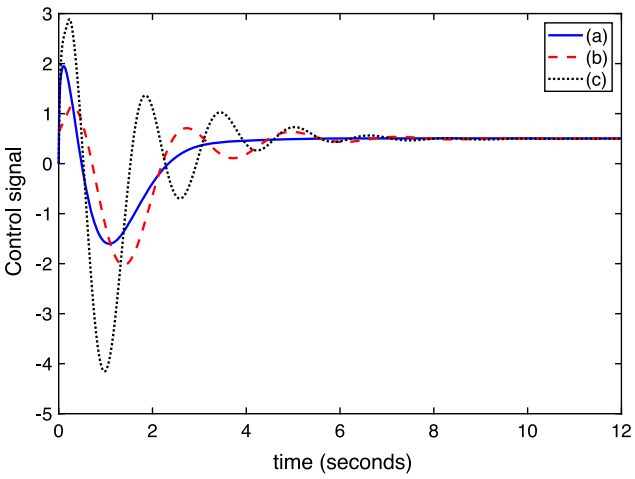

(b) Control signals

Fig. 9 Responses in Example-2, (a) Proposed, (b) Kumar et al. (2020) and (c) Begum et al. (2018)

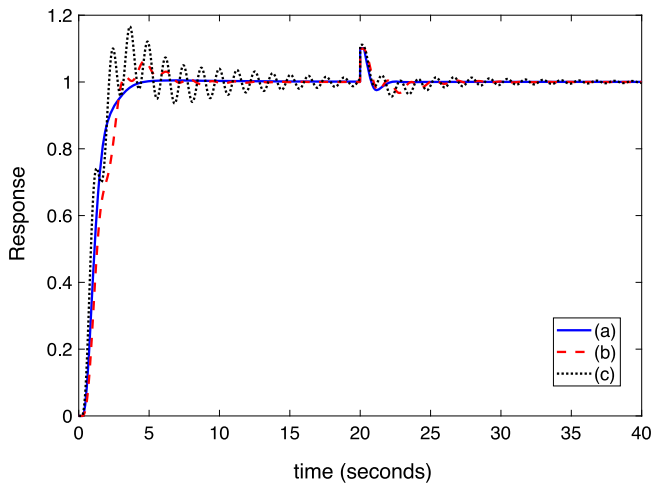

(a) Perturbation test 30% gain

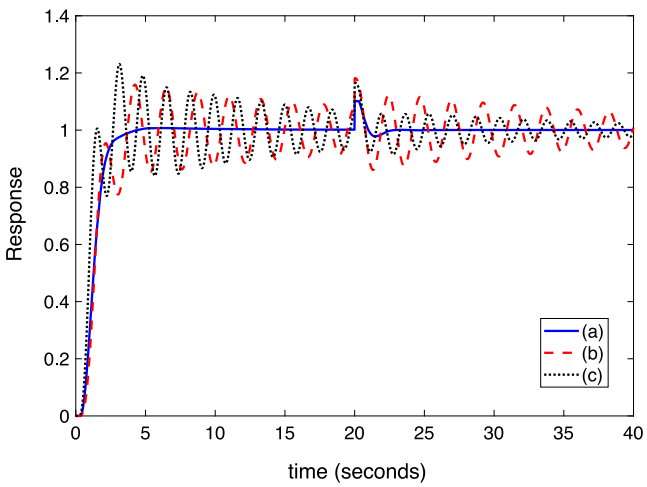

(b) Perturbation test 20% delay

Fig. 10 Perturbation test in Example-2, (a) Proposed, (b) Kumar et al. (2020) and (c) Begum et al. (2018)

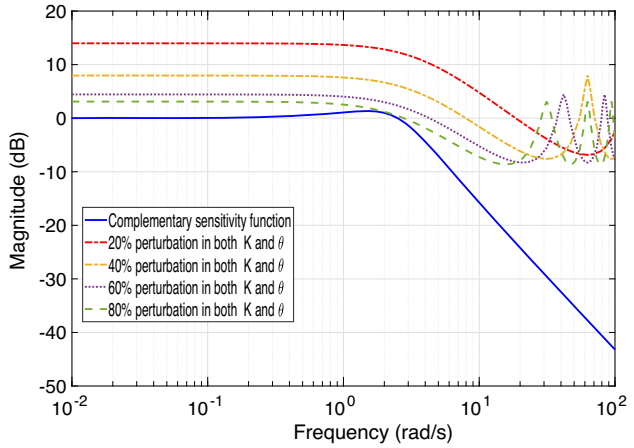

Fig. 11 Magnitude plot of the complementary sensitivity function and that of $1/((\Delta K/K+1)e^{-\Delta\theta s}-1$ for Example-2

Table 3 Performance comparison for Example-2

Tuning methods	t_s	A_p	ITSE	IAE	ITAE	ISE
Setpoint tracking						
Proposed	2.689	1.005	0.029	0.299	0.393	0.041
Kumar et al.	3.479	1.016	0.714	1.516	1.456	1.124
Begum et al.	3.387	1.073	0.152	0.493	1.185	0.070
Disturbance rejection						
Proposed	2.483	0.100	0.001	0.055	0.046	0.003
Kumar et al.	4.533	0.001	0.006	0.146	0.177	0.009
Begum et al.	4.718	0.100	0.004	0.123	0.158	0.007

and regulatory responses as well as control responses from the proposed design and other methods are shown in Fig. 13a

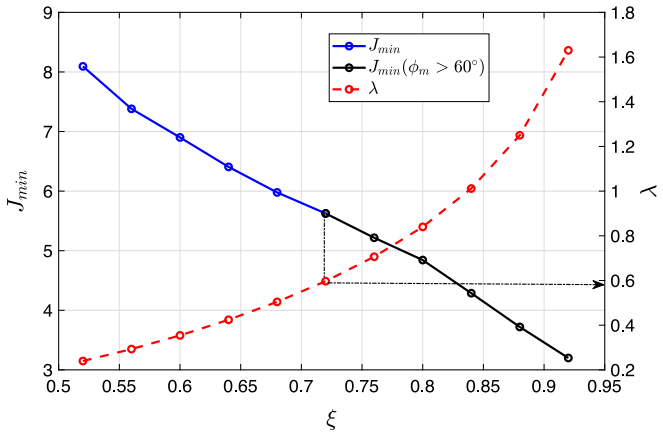

(a) Variation of λ and J_{min} with ξ for Example-3

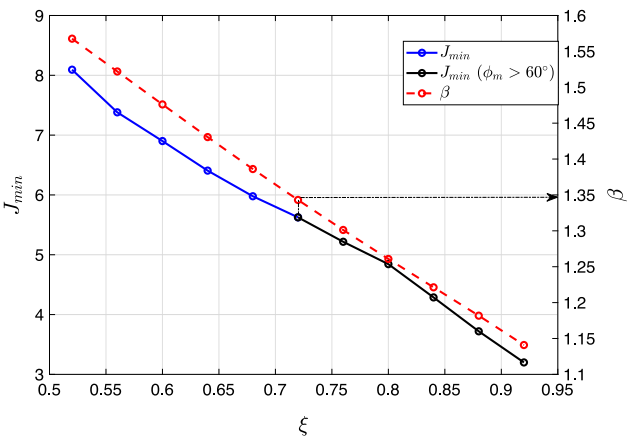

(b) Variation of β and J_{min} with ξ for Example-3

Fig. 12 Obtain the tuning parameters for Example-3

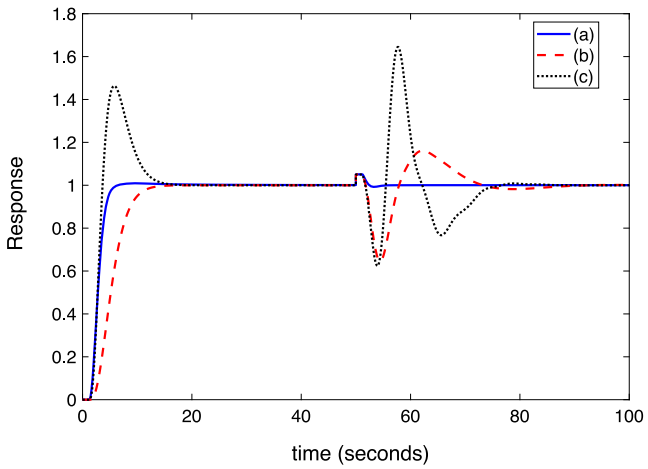

(a) Servo and Regulatory Responses

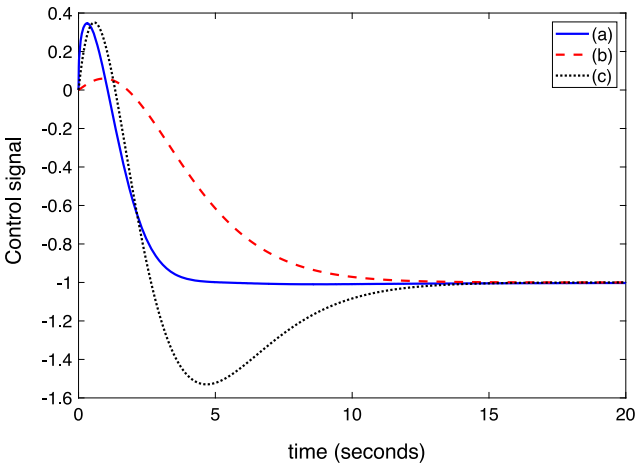

(b) Control signals

Fig. 13 Responses in Example-3, (a) Proposed, (b) Ajmeri and Ali (2017) and (c) Uma and Rao (2014)

Table 4 Performance comparison for Example-3

Tuning methods	t_s	A_p	ITSE	IAE	ITAE	ISE
Setpoint tracking						
Proposed	4.760	1.009	0.099	0.587	1.751	0.079
Ajmeri and Ali	10.021	0.997	0.625	1.285	7.296	0.161
Uma and Rao	11.925	1.463	4.662	3.747	14.545	1.928
Disturbance rejection						
Proposed	4.956	0.050	0.001	0.050	0.113	0.001
Ajmeri and Ali	21.441	0.354	0.677	1.144	10.712	0.092
Uma and Rao	22.915	0.646	9.080	3.359	38.020	1.013

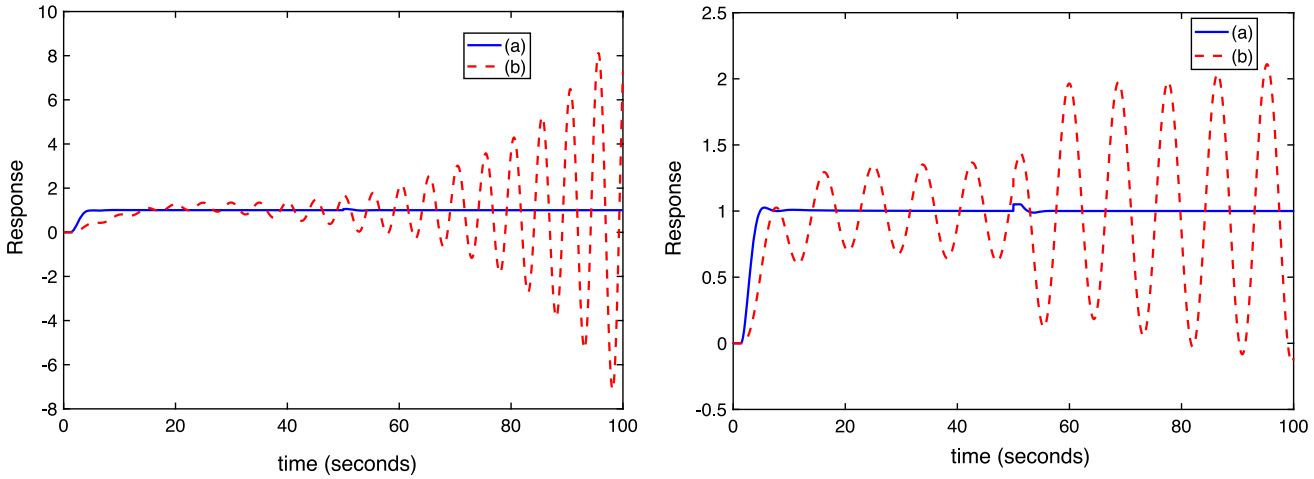

(a) Perturbation test 15% gain (b) Perturbation test 10% delay

Fig. 14 Perturbation test in Example-3, (a) Proposed and (b) Ajmeri and Ali (2017)

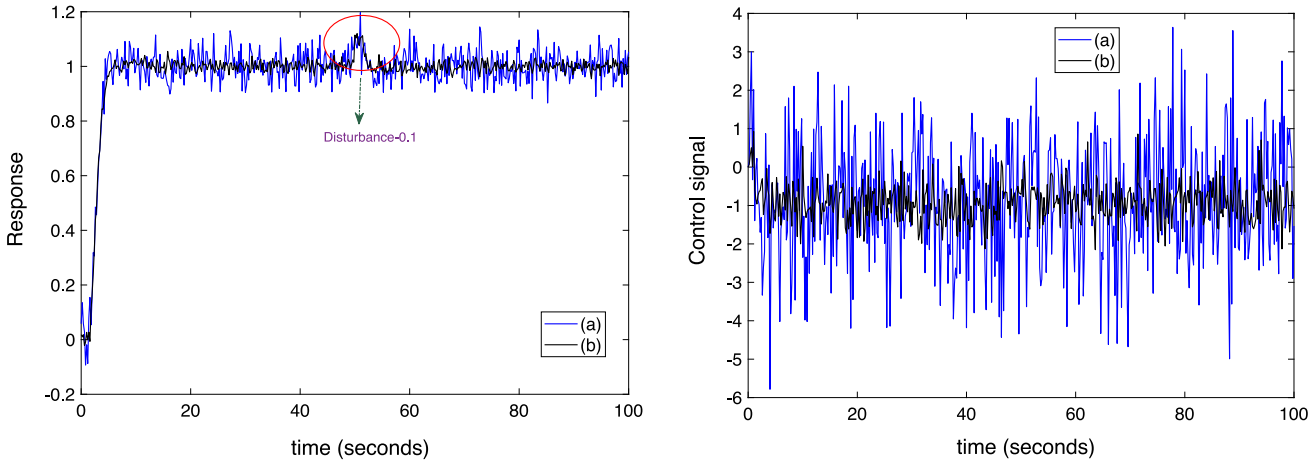

(a) Output Response (b) Control signal

Fig. 15 Response under noise (a) With SNR = 10 dB and (b) With SNR = 20 dB

and b. The result claimed the efficacy of the new structure from Table 4.

To analyze the robustness, perturbations of +15% in process gain and +10% perturbations in time delay are considered. The results are shown in Fig. 14a and b, respectively. The method proposed by Uma and Rao (2014) failed to satisfy the required perturbation and thus, their result was not shown. Again it is easy to claim the robustness from the presented method.

The measurement noise arises from measuring devices like sensors, other electric sources, control valves or the process itself. The signal-to-noise ratio (SNR) is a measure of the strength of the desired signal relative to background noise. The SNR is defined as SNR $= 10 \log \frac{{\sigma_y}^2}{{\sigma_n}^2}$, where ${\sigma_y}^2$ is the variance of output signal and ${\sigma_n}^2$ is the variance of noise. The results with noisy outputs having SNR of 10 dB and 20 dB using the proposed scheme are presented in Fig. 15a and b. Same time the external disturbance of 0.1 value was also added in the closed-loop control. It is proved from the analysis that the presented structure performs well with disturbance and measurement noise issues.

6.4 Example: 4

Let us take the recently studied process control example by Begum et al. (2020) as,

$$G_{p4}(s) = \frac{3.433}{103.1s - 1} e^{-20s}. \tag{43}$$

The presented scheme was compared with Begum et al. (2020) and Vanavil et al. (2014). In Begum et al. (2020), PID controller with settings $K_c = 1.249$, $T_i = 89.6$ and $T_d = 5.64$ was taken and for Vanavil et al. (2014), PID with lead-lag filter was shown with settings $K_c = 0.178$, $T_i = 13.333$, $T_d = 5.0$, $\alpha = 94.65$ and $\beta = 5.98$.

Following the presented tuning steps from Table 1, the parameters λ and β are estimated with values 4.653 and

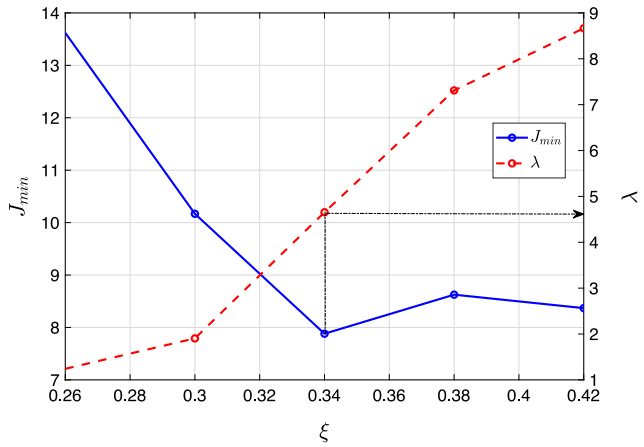

(a) Variation of λ and J_{min} with ξ for Example-4

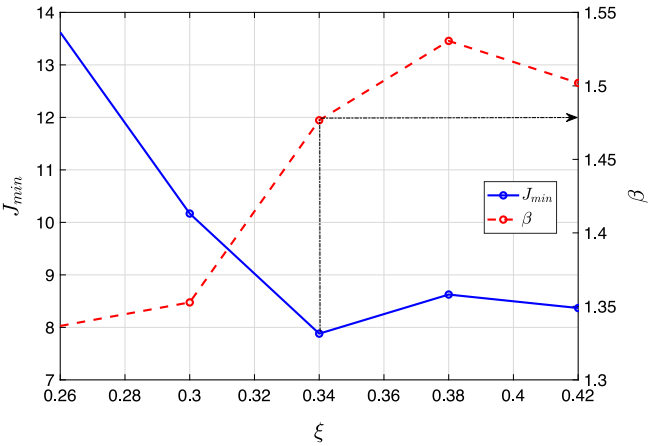

(b) Variation of β and J_{min} with ξ for Example-4

Fig. 16 Obtain the tuning parameters for Example-4

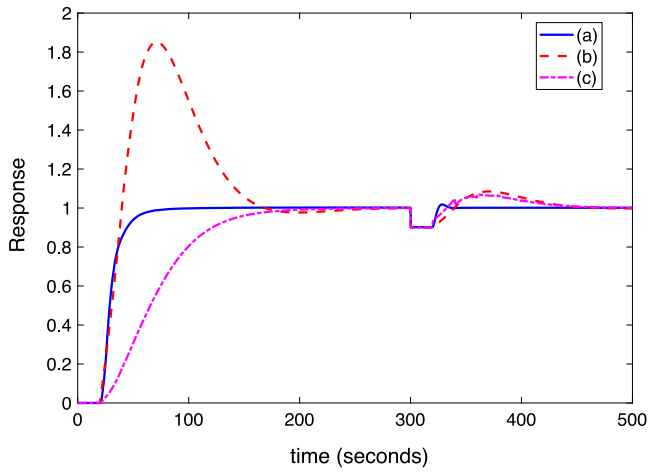

(a) Servo and Regulatory responses

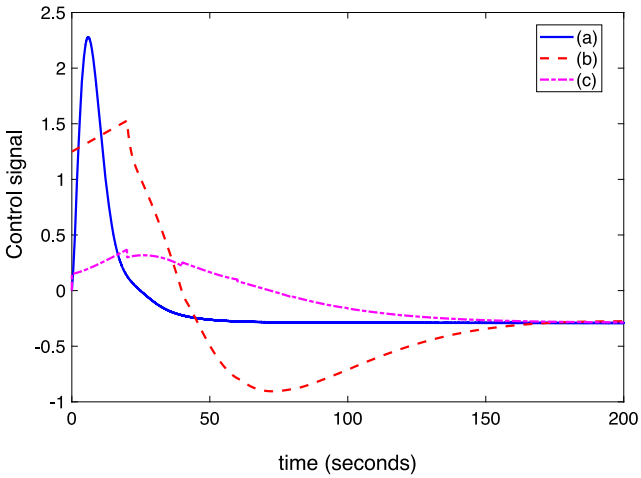

(b) The control signals

Fig. 17 Step responses in Example-4, (a) Proposed, (b) Begum et al. (2020) and (c) Vanavil et al. (2014)

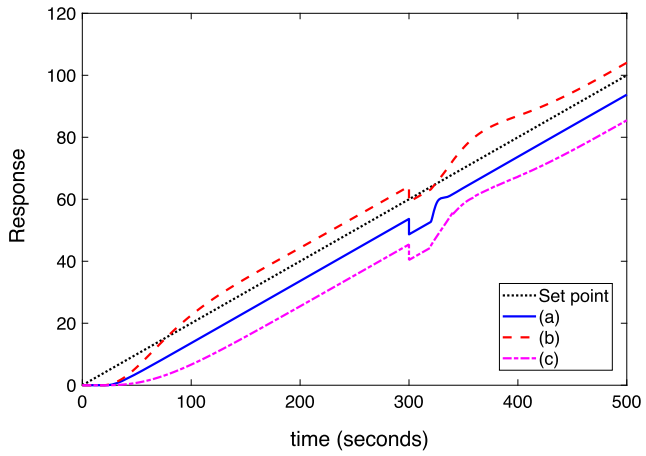

(a) Servo and Regulatory responses

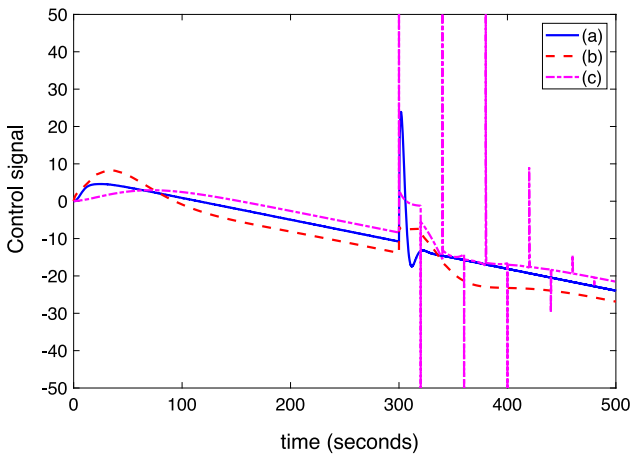

(b) The control signals

Fig. 18 Ramp responses in Example-4, (a) Proposed, (b) Begum et al. (2020) and (c) Vanavil et al. (2014)

Table 5 Performance comparison for Example-4

Tuning methods	t_s	A_p	ITSE	IAE	ITAE	ISE
Setpoint tracking						
Proposed	52.076	1.001	1.212	2.079	38.397	0.218
Begum et al	151.777	1.851	2.9e+03	83.177	4.92e+03	59.969
Vanavil et al	142.511	0.971	294.297	21.307	1.84e+03	3.347
Disturbance rejection						
Proposed	33.310	0.100	0.035	0.431	11.191	0.019
Begum et al	151.777	0.100	29.692	8.471	524.759	0.600
Vanavil et al	160.520	0.100	19.895	7.465	432.272	0.480

1.477, respectively. The stabilizer controller is set with gain value $K_{ps} = 2$. As seen from Fig. 16a and b, the performance constraint becomes $\xi = 0.34$ for the optimal cost function. Using the process model parameters and obtained

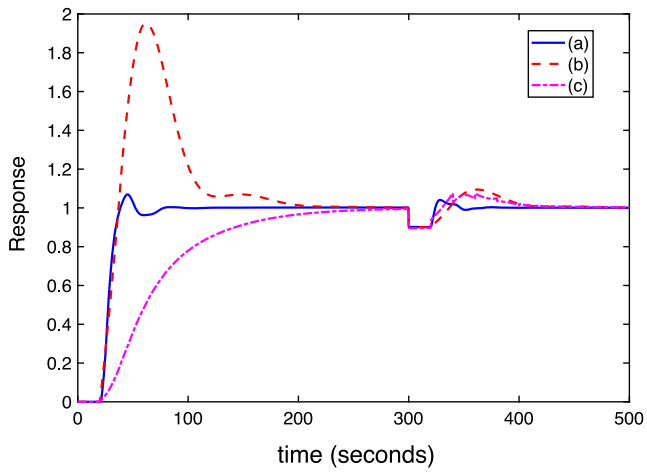

(a) Perturbation test 20% gain

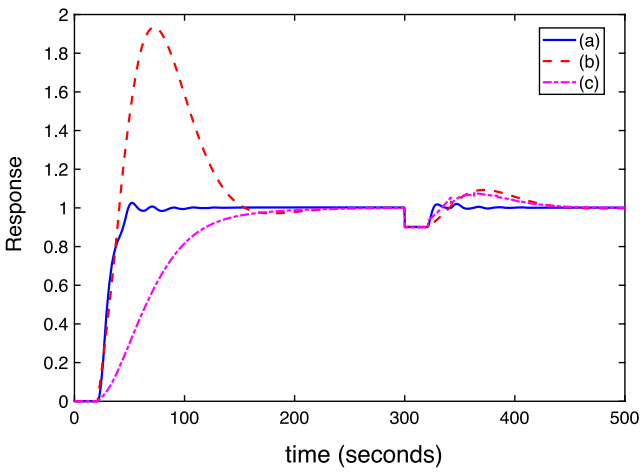

(b) Perturbation test 5% delay

Fig. 19 Perturbation test in Example-4, (a) Proposed, (b) Begum et al. (2020) and (c) Vanavil et al. (2014)

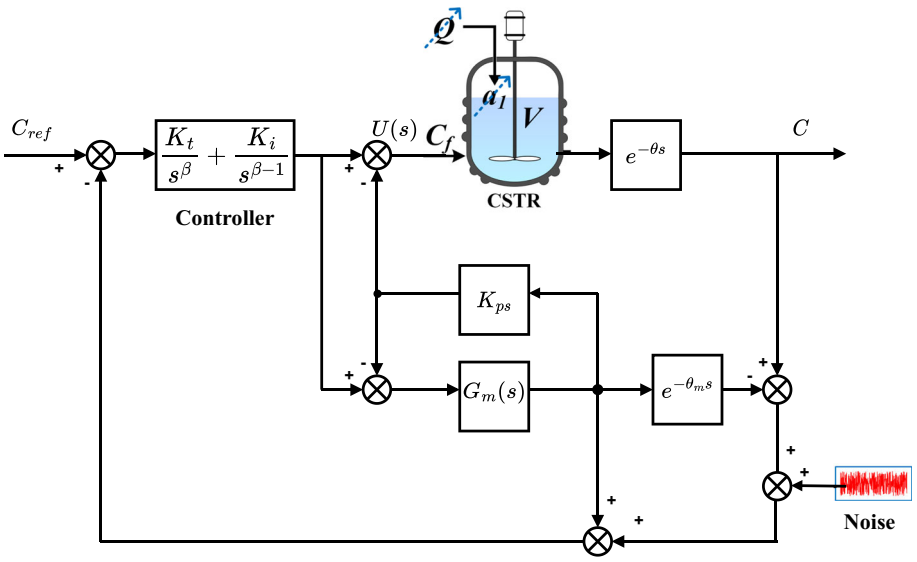

Fig. 20 Block diagram of CSTR using proposed scheme

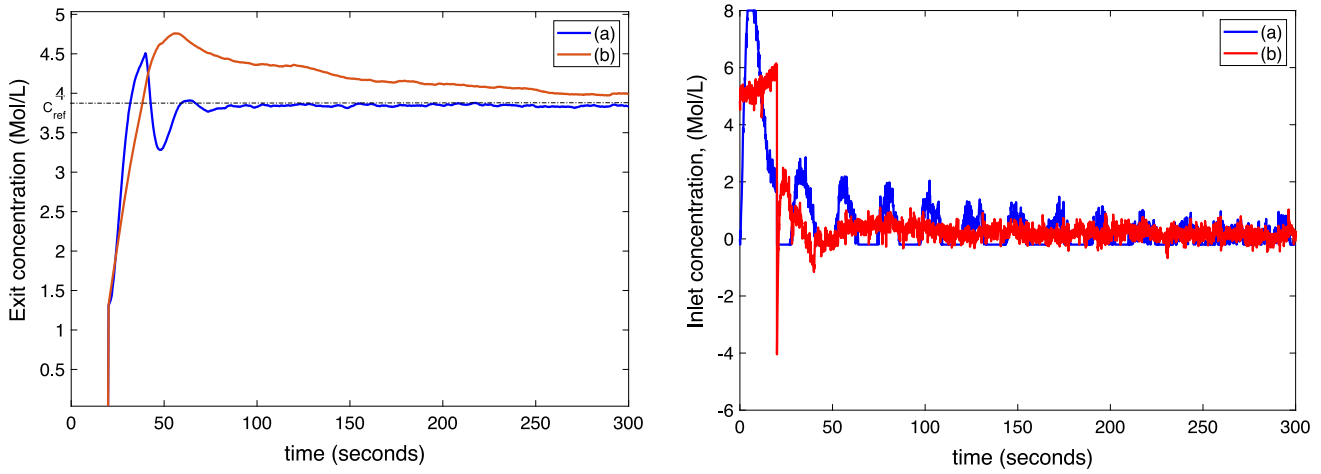

(a) Servo responses (b) The control signals

Fig. 21 Process output and control efforts for the nonlinear CSTR, (a) Proposed and (b) Begum et al. (2020)

λ and β, the fractional TI controller's gains are $K_t = 0.063$, $K_i = 6.454$, $\beta = 1.477$ and $\alpha = 0.476$. The set-point filter of the form $f_s = 1/(10\,s + 1)$ is also added to improve the setpoint smoothness. A negative step disturbance of 0.1 is given at the output side. The setpoint tracking and control input signals are shown in Fig. 17a and b, respectively, with results provided from other methods. Furthermore, an investigation was carried out with ramp reference signal of slope 0.2 at 0 s and negative step disturbance of 5 at 300 s. The corresponding results can be seen in Fig. 18a and b. It can be depicted that the presented method performed better than other controllers.

The same observation can be seen from the numerical values presented in Table 5. The robust performance is also observed by assuming a perturbation of 20% in process gain and 5% in process delay. Figure 19a and b are plotted for verification. Under this mismatch condition, the present tuning approach shows the robustness in terms of perturbed conditions.

6.4.1 Case Study on Nonlinear System

The proposed method was investigated on nonlinear Jacketed continuously stirred tank reactor (CSTR) system, and corresponding block diagram is shown in Fig. 20. The isothermal chemical CSTR exhibits multiple steady states. The reactor's mathematical model is given as

$$\frac{dC}{dt} = \left(\frac{Q}{V}\right)(C_f - C) - \left[\frac{K_1 C}{(K_2 C + 1)^2}\right] \tag{44}$$

where Q is the inlet flow rate, c_f is the inlet concentration, c is the reactor's exit concentration. The model parameters are given by $Q = 0.0333$ L/s, reactor volume $V = 1$L,

Table 6 Performance comparisons

Method	Structure	No. of Controllers / Filters	Summary of performance
Proposed	IMC-SP	4	Optimal Control signal Low performance indices Robust
Begum et al. (2020)	IMC	4	Large Control signal High performance indices Poor Disturbance test
Vanavil et al. (2014)	IMC	5	More controllers Optimal Control signal High performance indices Better tracking and load disturbance
Onat (2019)	PI-PD	4	Good performance indices Failed in perturbation test
Ozyetkin (2018)	FOPI-FOPD	4	Poor perturbation test Good performance indices Difficult tuning
Bingi et al. (2018)	PID	4	High ITSE and overshoot Oscillatory in perturbation test
Bingi et al. (2018)	FOPID	4	Sluggish response Overshoot in load disturbance Oscillatory in perturbation test
Kumar et al. (2020)	IMC	3	Good control signal Oscillatory in perturbation test
Begum et al. (2018)	IMC	5	High control signal Oscillatory in perturbation test
Ajmeri and Ali (2017)	SP	8	Many controllers Low control signal Oscillatory in perturbation test
Uma and Rao (2014)	SP	9	Many controllers Large control signal and overshoot Failed in perturbation test High performance indices

$K_1 = 10$L/s and $K_2 = 10$ L/mol. The desirable unstable steady state is obtained at $C = 1.316$ corresponding to the nominal value of $C_f = 3.288$ mol/L. The process has a dead time of 20 s and linearized (44) around the manipulated variable C. The signals C and C_f are plotted for a $C_{ref} = 3.9$ mol/L (steady-state). The impact of band limited white noise of amplitude 0.1 used to verify the robustness. The obtained process outputs and control signals are shown in Fig. 21a and b, respectively. It is worth noting that the IMC-SP can maintain the desired steady state even with noise.

6.5 The Comparison Table

From the comprehensive numerical studies and literature review, Table 6 is presented for the reference with key features and limitations of various approaches related to the unstable processes.

7 Conclusions

A modified IMC-SP setup for an unstable process was reported in this research. Despite the fact that the controller has a fractional-order integrator, derivative, and SP, a simple method is established. The tuning method resulted in a significant improvement in setpoint tracking after changing controller settings from the predicted cost function. This design works in the presence of parameter fluctuations, external load disturbance, and measurement noise. The numerical analysis revealed that the strategy is fairly simple

while outperforming previous approaches. In a closed-loop performance comparison, the proposed tuning is proven to be superior to other documented techniques developed for isothermal chemical continuous stirred tank reactors. Further research on higher-order, non-minimum phase, and fractional-order type unstable models can be conducted as an appropriate extension of the proposed methodology.

Declarations

Conflicting Interests The author(s) declared no potential conflicts of interest with respect to the research, authorship, and/or publication of this article.

References

Ahmed, M., Magdy, G., Khamies, M., & Kamel, S. (2022). Modified TID controller for load frequency control of a two-area interconnected diverse-unit power system. *International Journal of Electrical Power and Energy Systems, 135*, 107528. https://doi.org/10.1016/j.ijepes.2021.107528

Ajmeri, M., & Ali, A. (2017). Analytical design of modified smith predictor for unstable second-order processes with time delay. *International Journal of Systems Science, 48*(8), 1671–1681. https://doi.org/10.1080/00207721.2017.1280554

Begum, K. G. (2022). Design of a simple control strategy for time-delayed unstable series cascade processes. *Arabian Journal for Science and Engineering, 47*, 6679–6691. https://doi.org/10.1007/s13369-022-06650-7

Begum, K. G., Rao, A., & Radhakrishnan, T. (2017). Enhanced IMC based PID controller design for non-minimum phase integrating processes with time delays. *ISA Transactions, 68*, 223–234. https://doi.org/10.1016/j.isatra.2017.03.005

Begum, K. G., Rao, A. S., & Radhakrishnan, T. (2018). Optimal controller synthesis for second order time delay systems with at least one RHP pole. *ISA Transactions, 73*, 181–188. https://doi.org/10.1016/j.isatra.2017.12.025

Begum, K. G., Rao, A., & Radhakrishnan, T. (2020). Novel IMC filter design-based PID controller design for systems with one right half plane pole and dead-time. *International Journal of Automation and Control, 14*(4), 423–444. https://doi.org/10.1504/IJAAC.2020.10029539

Bilal, H., Yao, W., Guo, Y., Wu, Y., & Guo, J. (2017). Experimental validation of fuzzy PID control of flexible joint system in presence of uncertainties. In *2017 36th Chinese Control Conference (CCC)* (pp. 4192–4197). https://doi.org/10.23919/ChiCC.2017.8028015

Bilal, H., Yin, B., Aslam, M. S., Anjum, Z., Rohra, A., & Wang, Y. (2023). A practical study of active disturbance rejection control for rotary flexible joint robot manipulator. *Soft Computing, 27*, 4987–5001. https://doi.org/10.1007/s00500-023-08026-x

Bilal, H., Yin, B., Kumar, A., Ali, M., Zhang, J., & Yao, J. (2023). Jerk-bounded trajectory planning for rotary flexible joint manipulator: an experimental approach. *Soft Computing, 27*, 4029–4039. https://doi.org/10.1007/s00500-023-07923-5

Bingi, K., Ibrahim, R., Karsiti, M. N., Hassan, S. M., & Harindran, V. R. (2018). A comparative study of 2DOF PID and 2DOF fractional order PID controllers on a class of unstable systems. *Archives of Control Sciences, 28*(4), 635–682. https://doi.org/10.24425/acs.2018.125487

Dwivedi, P., & Pandey, S. (2021). Tuning rules: Graphical analysis and experimental validation of a simplified fractional order controller for a class of open-loop unstable systems. *Asian Journal of Control, 23*(5), 2293–2310. https://doi.org/10.1002/asjc.2635

Gengjin, S., Zhiqiang, G., YangQuan, C., Donghai, L., & Yanjun, D. (2022). A controller design method for high-order unstable linear time-invariant systems. *ISA Transactions, 130*, 500–515. https://doi.org/10.1016/j.isatra.2022.04.012

Guha, D., Roy, P. K. R., & Banerjee, S. (2019). Maiden application of SSA-optimized CC-TID controller for load frequency control of power systems. *IET Generation, Transmission & Distribution, 13*(7), 1110–1120. https://doi.org/10.1049/iet-gtd.2018.6100

Karan, S., & Dey, C. (2020). Simplified tuning of IMC based modified Smith predictor for UFOPDT processes. *Chemical Product and Process Modeling, 16*(1), 21–40. https://doi.org/10.1515/cppm-2019-0132

Kumar, D., & Raja, G. L. (2022). Unified fractional indirect IMC-based hybrid dual-loop strategy for unstable and integrating type CSTRs. *International Journal of Chemical Reactor Engineering, 21*(3), 251–272. https://doi.org/10.1515/ijcre-2022-0120

Kumar, M., & Hote, Y. V. (2020). Robust PIDD2 controller design for perturbed load frequency control of an interconnected time-delayed power systems. *IEEE Transactions on Control Systems Technology, 29*(6), 2662–2669. https://doi.org/10.1109/TCST.2020.3043447

Kumar, M., Prasad, D., & Singh, R. (2020). Performance enhancement of IMC-PID controller design for stable and unstable second-order time delay processes. *Journal of Central South University, 27*, 88–100. https://doi.org/10.1007/s11771-020-4280-7

Kumari, S., Aryan, P., & Raja, G. L. (2021). Design and simulation of a novel FOIMC-PD/P double-loop control structure for CSTRs and bioreactors. *International Journal of Chemical Reactor Engineering, 19*(12), 1287–1303. https://doi.org/10.1515/ijcre-2021-0140

Lurie, B. (1994). Three parameters tunable Tilt-Integral Derivative (TID) controller US Patent US5371670.

Mehta, U., & Kaya, I. (2017). Smith predictor with sliding mode control for processes with large dead times. *Journal of Electrical Engineering, 68*(6), 463–469. https://doi.org/10.1515/jee-2017-0081

Mehta, U., & Rojas, R. (2017). Smith predictor based sliding mode control for a class of unstable processes. *Transactions of the Institute of Measurement and Control, 39*(5), 706–714. https://doi.org/10.1177/0142331215619973

Mehta, U., Aryan, P., & Raja, G. L. (2023). Tri-parametric fractional-order controller design for integrating systems with time delay. *IEEE Transactions on Circuits and Systems II: Express Briefs*. https://doi.org/10.1109/TCSII.2023.3269819

Nath, U. M., Dey, C., & Mudi, R. (2021). Review on IMC based PID Controller Design Approach with Experimental Validations. *IETE Journal of Research, 69*(3), 1640–1660. https://doi.org/10.1080/03772063.2021.1874839

Onat, C. (2019). A new design method for PI-PD control of unstable processes with dead time. *ISA Transactions, 84*, 69–81. https://doi.org/10.1016/j.isatra.2018.08.029

Ozyetkin, M. M. (2018). A simple tuning method of fractional order PI^{λ}-PI^{μ} controllers for time delay systems. *ISA Transactions, 74*, 77–87. https://doi.org/10.1016/j.isatra.2018.01.021

Padula, F., & Visioli, A. (2015). Advances in Robust Fractional. *Control*. https://doi.org/10.1007/978-3-319-10930-5

Pashaei, S., & Bagheri, P. (2020). Parallel cascade control of dead time processes via fractional order controllers based on Smith predictor. *ISA Transactions, 98*, 186–197. https://doi.org/10.1016/j.isatra.2019.08.047

Raja, G. L., & Ali, A. (2021). New PI-PD Controller Design Strategy for Industrial Unstable and Integrating Processes with Dead Time and Inverse response. *Journal of Control, Automation and Elec-*

trical Systems, 32(8), 266–280. https://doi.org/10.1007/s40313-020-00679-5

Rakesh, B., Maghade, D. K., Sondkar, S., & Pawar, S. N. (2021). A review of PID control, tuning methods and applications. *International Journal of Dynamics and Control, 9*, 818–827. https://doi.org/10.1007/s40435-020-00665-4

Ranjan, A., & Mehta, U. (2022). Fractional filter IMC-TDD controller design for integrating processes. *Results in Control and Optimization, 8*, 100155. https://doi.org/10.1016/j.rico.2022.100155

Ranjan, A., & Mehta, U. (2023). Fractional internal-model-control filter-based controller tuning for series cascade unstable plants. *International Journal of Dynamics and Control*. https://doi.org/10.1007/s40435-023-01162-0

Ranjan, A., & Mehta, U. (2023). Improved control of integrating cascade processes with time delays using fractional-order IMC with Smith predictor. *Proceedings of the Institution of Mechanical Engineers. Part I: Journal of Systems and Control Engineering*. https://doi.org/10.1177/09596518231168510

Ranjan, A., Mehta, U., & Saxena, S. (2023). A comprehensive review of modified Internal Model Control (IMC) structures and their filters for unstable processes. *Annual Reviews in Control*. https://doi.org/10.1016/j.arcontrol.2023.04.006

Rao, A. S., & Manickam, C. (2008). Analytical design of modified Smith predictor in a two-degrees-of-freedom control scheme for second order unstable processes with time delay. *ISA Transactions, 47*, 407–419. https://doi.org/10.1016/j.isatra.2008.06.005

Saxena, S., & Biradar, S. (2022). Fractional-order IMC controller for high-order system using reduced-order modelling via Big-Bang, Big-Crunch optimisation. *International Journal of system science, 53*(1), 168–181. https://doi.org/10.1080/00207721.2021.1942587

Shamsuzzoha, M., & Lee, M. (2008). Analytical design of enhanced PID filter controller for integrating and first order unstable processes with time delay. *Chemical Engineering Science, 63*(10), 2717–2731. https://doi.org/10.1016/j.ces.2008.02.028

Somefun, O. A., Akingbade, K., & Dahunsi, F. (2021). The dilemma of PID tuning. *Annual Reviews in Control, 52*, 65–74. https://doi.org/10.1016/j.arcontrol.2021.05.002

Tan, W., Marquez, H. J., & Chen, T. (2003). IMC design for unstable processes with time delays. *Journal of Process Control, 13*(3), 203–213. https://doi.org/10.1016/S0959-1524(02)00058-6

Uma, A., & Rao, A. S. (2014). Enhanced modified Smith predictor for second-order non-minimum phase unstable processes. *International Journal of Systems Science, 47*(4), 966–981. https://doi.org/10.1080/00207721.2014.911385

Vanavil, B., Anusha, A. V. N. L., Perumalsamy, M., & Rao, A. S. (2014). Enhanced IMC-PID controller design with lead-lag filter for unstable and integrating processes with time delay. *Chemical Engineering Communications, 201*(11), 1468–1496. https://doi.org/10.1080/00986445.2013.818983

Vavilala, S. K., Thirumavalavan, V., & Chandrasekaran, K. (2020). Level control of a conical tank using the fractional order controller. *Computers & Electrical Engineering, 87*, 106690. https://doi.org/10.1016/j.compeleceng.2020.106690

Zhong-Ping, J., & Tengfei, L. (2018). Small-gain theory for stability and control of dynamical networks: A Survey. *Annual Reviews in Control, 46*, 58–79. https://doi.org/10.1016/j.arcontrol.2018.09.001